# Deliverable 2.3: Process limits diamond processing

## Dissemination level: Public version


**Owner**

**Name:** Noemie Dury

**Lead Beneficiary:** Class 4 Laser Professional

**Phone:** +41 32 384 49 55

**E-mail:** Noemie.dury@class4laser.ch


**Context**

**Author(s):** Element Six: William Scalbert

**Work Package:** WP2

**Task:** T2.3

**Document Status**

**Version:** 1.00

**Last modified:** 13/03/2018

**Status:** Final

**Approved by:** Marwan Abdou-Ahmed, USTUTT

**Date Approved:** 26/04/2018

**Declaration:** Any work or result described therein is genuinely a result of the Hiperdias project. Any other source will be properly referenced where and when relevant

# Contents

1 Scope ........ 3
2 Introduction ........ 4
3 Experimental set up for ablation trials ........ 5
4 Influence of Heat Accumulation ........ 6
4.1 Increase of ablation rate with heat accumulation ........ 6
4.2 Critical surface damage with heat accumulation ........ 7
5 Variation of Ablation Rate with PCD Grades ........ 8
5.1 PCD grades ........ 8
5.2 Ablation rate variation with fluence ........ 9
5.3 Grain size influence ........ 10
5.4 Diamond composition influence ........ 10
6 Graphitization of Diamond under Ultra-Short Pulsed Ablation ........ 10
6.1 Raman spectroscopy analyses ........ 10
6.2 Standard Raman Spectrometer Measurements ........ 11
6.3 Micro Raman Spectrometer Measurements ........ 13
7 Conclusion ........ 14
8 References ........ 15

# 1 Scope

This deliverable presents the tests carried out to understand fundamental laser ablation process of PCD material. KPIs were previously defined in deliverable D1.3 to determine productivity and quality parameters to be achieved by laser ablation process (Tab.1). The objective in this deliverable is to determine key parameters of the PCD laser ablation mechanism resulting in highest productivity and highest quality with these KPIs as targets. The fundamental understanding of the PCD materials ablation process with ultra-short pulses provides data to determine final specifications of the different parts of the ultra-fast high power system: laser source, scanning system, beam delivery system, hardware, software, etc... As the development of the high power laser is ongoing, tests were performed with a low power ultra-short pulsed laser (cf. laser specifications in part 4). Therefore, tests were carried out with the objective to measure evolution of the ablation process with average power increases to forecast behavior at high power. This process development work demonstrated some limitations in the process.

*Table 1. List of Element Six'KPIs regarding diamond laser polishing process – Top: production related KPIs. Bottom: quality related KPIs*

| No | KPI | KPI Values for success | Validation Status |
|---|---|---|---|
| **1** | **Material Removal Rate** | Expected : > 0.150 $mm^3/s$ per disc | |
| | | Validated : > 0.075 $mm^3/s$ per disc | |
| **2** | **Total Handling Time** | Expected : < 10 min per disc | |
| | | Validated : < 20 min per disc | |
| | | Non validated : > 20 min per disc | |
| **3** | **Post Processing/Cleaning Time** | Expected : no post processing | |
| | | Validated : quick surface cleaning | |
| | | Non validated : No additional work/cost | |

| No | KPI | KPI Values for success | Validation Status |
|---|---|---|---|
| **5** | **Surface Roughness** | Expected : Sa < 0.010 µm, Sz < 0.12 µm (1) | |
| | | Validated : Ra < 0.100 µm (2) | |
| | | Non validated : Ra > 0.100 µm | |
| **6** | **Shape deviation (3)** | Expected : < +/- 2 µm | |
| | | Validated : < +/- 5 µm | |
| | | Non validated : > +/- 5 µm | |
| **7** | **Visual Defects (4)** | Expected : pass rate 100% | |
| | | Validated : pass rate > 90% | |
| | | Non validated : pass rate < 90% | |
| **9** | **Graphitization (5)** | Expected : No micro-structure modification | |

# 2 Introduction

Former developments of laser ablation processes to machine PCD material with femtosecond laser source have been analyzed[1,2,3]. The developed processes are generally focused on the laser ablation and laser machining of cutting tools for purposes like: cutting of the tip to near final size after brazing on the tool blank, ablation of the clearance face for surface smoothing, shaping of chip breakers on the rake face, etc... The objectives of these new laser processes are to replace conventional grinding processes and the focus is primarily on reaching the lowest surface roughness achievable by laser ablation. Results join to confirm that ultra-short pulses achieve greater surface finish with lower surface roughness. Those studies support the utilization of femtosecond laser pulses to produce the highest surface quality finish on PCD wafer material.

Fundamental investigation of laser ablation with ultra-short pulses have been done on various materials by Neuenschwander and al.[4-7]. These studies corroborate the role of the pulse length on the surface roughness, shorter pulses achieve higher surface quality, but also characterize its effect on the ablation rate. In general, higher removal efficiency with ultra-fast lasers is measured after ablation with shorter pulse lengths. The impact of shorter pulses is smaller on PCD than other materials like metals. But, in conclusion, shorter pulse length has two benefits on ultra-short pulsed ablation of PCD: a better surface finish is performed at a higher ablation rate.

In the scope of D1.2 to establish specifications of the process and the laser system, tests confirmed the ablation behavior of PCD material in relation to the pulse duration as stated by Neuenschwander and al. The goal was to state how critical the pulse length is on the process efficiency at low power to forecast effect at high power. An increase of the PCD removal rate was measured when pulse length is reduced from picosecond down to femtosecond (Fig.1). Additionally, these measurements highlighted the effect of the average power: the ablation rate slightly increases by reduction of pulse length from picosecond down to femtosecond below 2W, and this increase becomes more and more pronounced below 500fs when average power increases over 2W. This effect can be expected to be more important at high power.

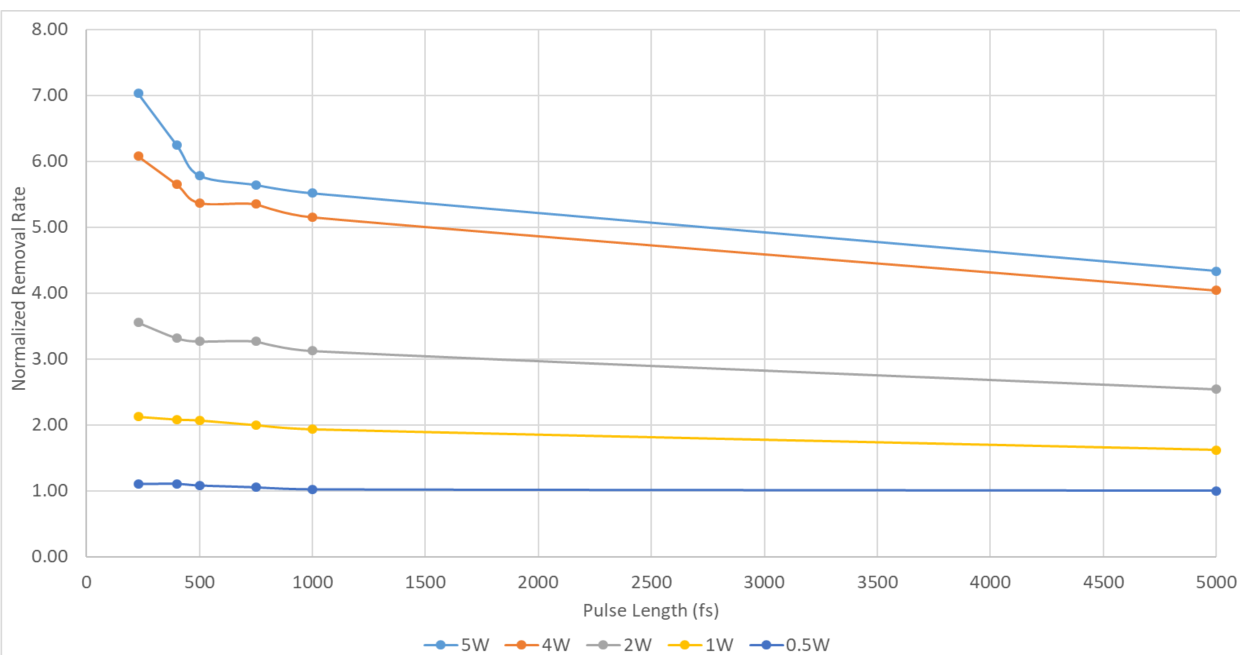


*Figure 1. Variation of ablation rate with the pulse length at different average powers*

In this deliverable D2.3, studies have been focused on the relationship between the ablation rate and the fluence, and the influence of the average power regarding heat accumulation[8,9]. The goal is to determine optimal fluence to achieve highest ablation rate without generating critical surface damage. After determination of the optimal of fluence, spot size to be achieved by final system have been calculated to perform highest ablation rate and surface quality with final system as defined by KPIs. Finally, graphitization of the diamond material after laser exposition was analyzed by Raman spectroscopy to qualify the influence of ultra-short pulsed laser process on material integrity.

# 3 Experimental set up for ablation trials

Laser ablation trials are undertaken with a Carbide laser from Light Conversion, characteristics of this laser are given in the chart below (Tab.2):

*Table 2. Characteristics of the laser used for the ablation trials*

| | |
|---|---|
| Wavelength | 1030nm |
| Pulse length | 230fs – 10ps |
| Maximum average power | 5W |
| Frequency | 60kHz – 1MHz |
| Polarization | Linear |
| $M^2$ | < 1.2 |

For beam delivery a Galvanometer scanning device fitted with a telecentric focal lens have been used to focus and move laser beam on the PCD top surface. Conventional CNC stages (X, Y, Z) have been used to allow linear movements for successive ablation trials and for positioning of the PCD top surface in focus. The experimental set up is presented in Figure 2:

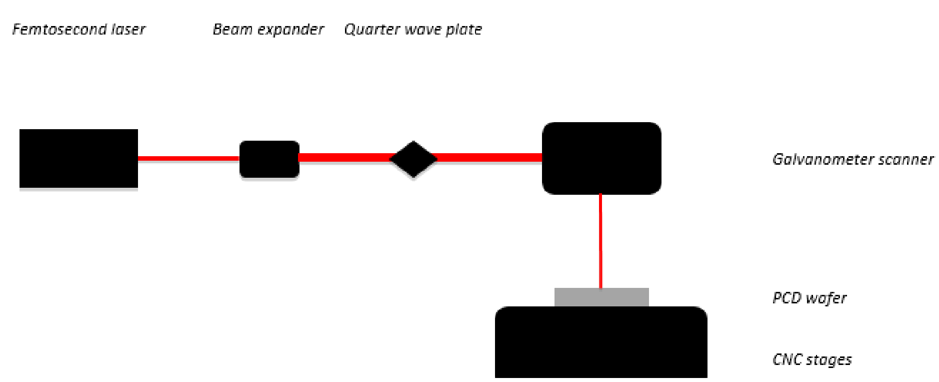


*Figure 2. Schematic of the laser system used for preliminary tests*

Ablation trials consist of ablating 3mm x 3mm squares into PCD materials with various diamond grain size and composition as outlined in Table 2. The ablation time is adjusted to achieve the same depth into the

PCD material. No Z stage movement is set up to maintain focal position as ablation rate varies from one sample to another. The laser spot focal position is set on the sample's top surface; therefore, the defocusing effect is constant for every square.
Variation of scanning parameters have been scanning speed and hatching distance. These two parameters set the spot overlap in both x and y directions of the scanner. A high spot overlap can generate heat accumulation during the ablation process[10]. Repetition of femtosecond laser pulses on the same surface location can produce accumulation of heat and a modification of the material removal process. The influence of the overlap is first analyzed to set the scanning parameters for the next trials in order to ensure no heat accumulation occurs and influences the following trials. For these tests, the laser parameters are set at the maximum value of average power and fluence, parameters which are most likely to generate heat accumulation in the material, and at the lowest pulse length 230fs which is the parameter likely to be used for final polishing process. Then scanning speed and hatching distance are modified to change the overall overlap from 25% to 95%.
After, as explained in previous chapter, studied laser parameters are the pulse length firstly and the fluence secondly, both studied at different average power. First, the pulse length is raised from 230fs up to 5ps with a fluence set over the ablation threshold and an overlap set at 55% (cf. Part 4). Experiments on the pulse length are applied from 0.5W to 5W to the Material 1 only. Second, the normalized fluence is modified from 1.01 to 16.75 at 3W, 1.36 to 22.83 at 4W and from 1.70 to 30.22 at 5W by changing the frequency while overlap is kept around 55% at low frequency and below 90% at high frequency. Pulse length was set up below 500fs (cf. Part 5). Experiments were repeated on the three mentioned PCD grades (Material 1, Material 2 and Material 3).

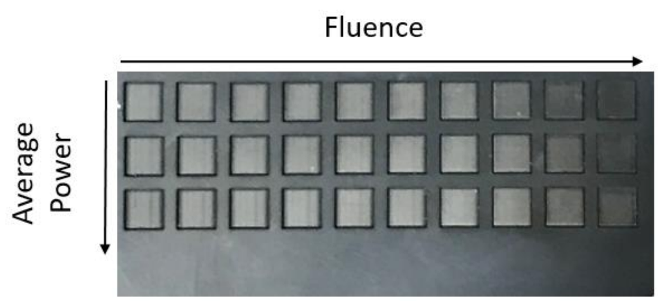


*Figure 3. Ablation trials on Material 1 (1µm grain size, 80% wt diamond content): variation of fluence with average power. These ablation trials were repeated on Material 2 and Material 3*

# 4 Influence of Heat Accumulation

## 4.1 Increase of ablation rate with heat accumulation

The study of the influence of the overall overlap (in x and y directions) at 230fs reveals some heat accumulation effect even though pulses are ultra-short (Fig.4). Removal rate remains constant for spot overlaps between 25% and 85% whereas it suddenly rises over at 95% spot overlap. This observation emphasizes the heat accumulation possibility when spots overlap at a high ratio even at 230fs.

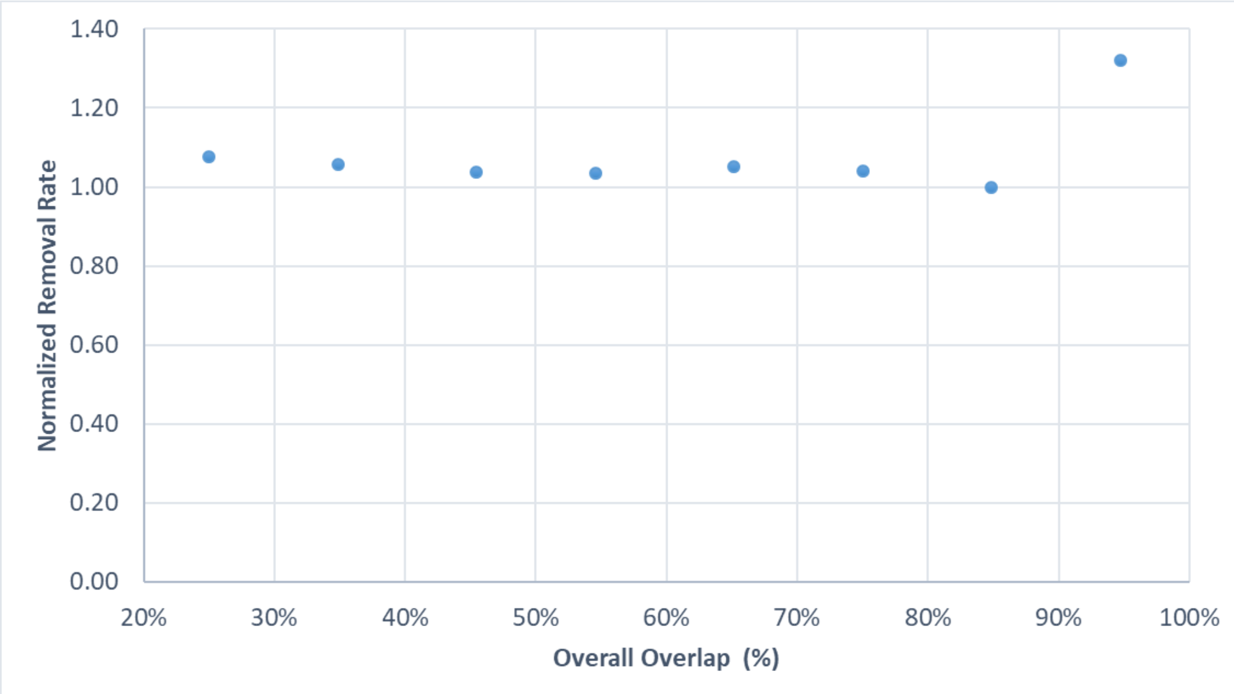


*Figure 4. Variation of the removal rate with the overall beam spot overlap for Material 1 (1µm grain size, 80% wt diamond content)*

These results highlights that heat accumulation effects increase the ablation rate. Potentially pulse bursts could increase ablation rate as pulse burst would generate heat accumulation effects. Pulse burst mode has been requested on high power laser from Amplitude Systems in D1.2 to test this theory.

## 4.2 Critical surface damage with heat accumulation

A high increase of ablation has been measured at 95% overlap, however visually the surface looks highly deteriorated (pictures on Fig.5). Sa value measurements confirm this observation: Sa is between 0.4µm and 0.6µm for overlaps below 85% and reaches 2.6µm at an overlap of 95%. The surface suffers from critical thermal damage at 95% overlap. Heat accumulation effects must be controlled to perform higher ablation rate while limiting thermal damage on the surface. Implementation of high frequency in the megahertz is required on final system to prevent from important thermal damage.

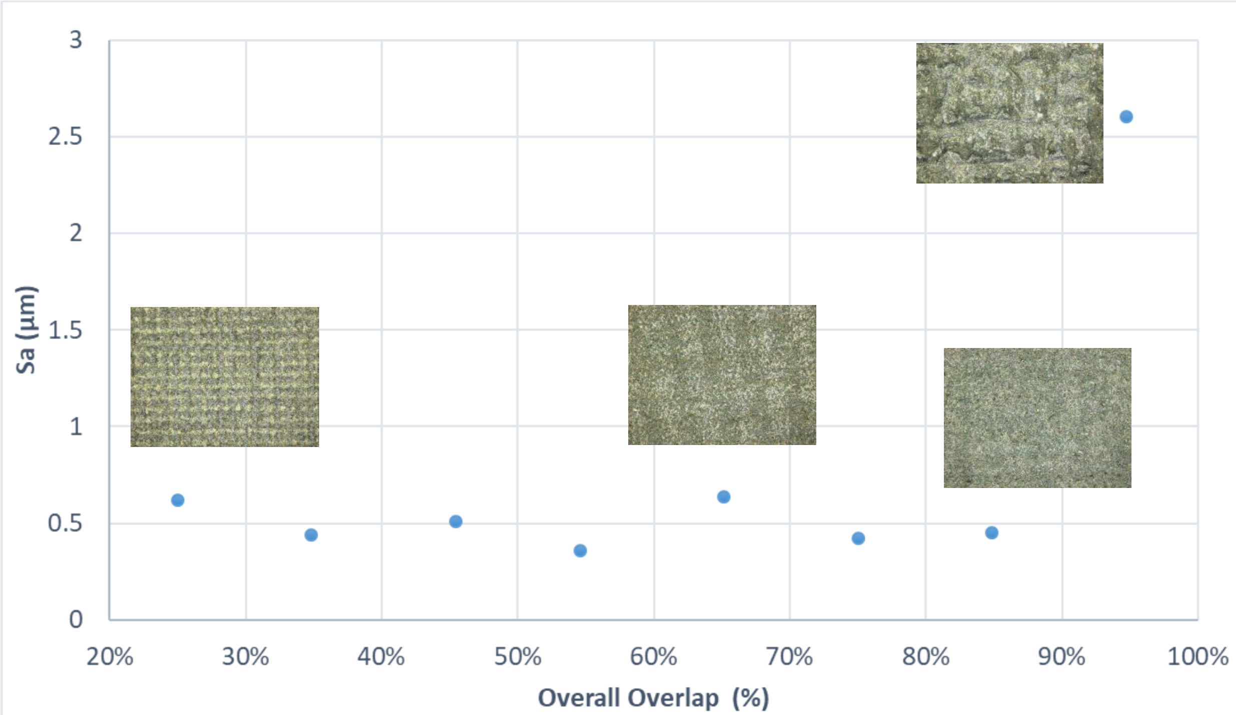


*Figure 5. Variation of Sa value with the overall beam spot overlap for Material 1 (1µm grain size, 80% wt diamond content); pictures taken with optical microscope x50*

For following trials, overlap is maintained at a value lower than 90% to avoid critical surface damage due to heat accumulation effects.

# 5 Variation of Ablation Rate with PCD Grades

## 5.1 PCD grades

A review of the literature regarding the interaction between ultra-short pulse and PCD material suggests that chemical composition and structure are not taken into account. The diamond grain size, binder composition and ratio diamond grain/binder can vary and form different specific PCD grades. Table 3 shows three examples of common industrial PCD grades produced by Element Six with cobalt as the binder material. The influence of the PCD chemical composition and structure is measured relative to the laser ablation with nanosecond pulses by Pacella and Butler-Smith[11,12]. They describe chemical composition and structure variations after the laser ablation process with nanosecond pulses. As the laser polishing process will potentially be applied to several PCD grades industrially, there is a need to characterize the role of PCD composition and structure regarding ultra-short pulsed laser ablation. For this purpose, three different PCD grades are tested to measure influence of fluence on ablation rate on the following trials: these grades present the highest variations of diamond grain size and diamond/binder ratios in the range of available products from Element Six for valuable comparison (Tab.3).

*Table 3. Chart of the PCD grades used for preliminary tests*

| PCD Grade Name | Average Grain Size (µm) | Diamond Content (wt %) | Cobalt Content (wt%) |
|---|---|---|---|
| Material 1 | 1 | 80 | 20 |
| Material 2 | 12 | 90 | 10 |
| Material 3 | 30 | 90 | 10 |

## 5.2 Ablation rate variation with fluence

Ablation rate is measured on three PCD grades at 3W, 4W and 5W for normalized fluence from 1.01 to 30.22, all measurements are reported on Figure 6.

First, a maximum ablation rate is observable at every average power for every type of PCD material. These maximum removal of material are achieved at one value of fluence which can be determined from the figure 4, confirming results Neuenschwander and al. for various PCD grades.

Second, it is very clear that the ablation rate of PCD material strongly variates according to its composition. At same parameters, up to a normalized fluence of 15, the ablation rate is the lowest on Material 3, higher on Material 2 and finally the highest on Material 1. This difference can directly be linked to the grain size: Material 3 and Material 2 only have a difference in grain size (both have same diamond percentage). For high normalized fluence over 15, ablation rate of Material 1 becomes lower than for Material 2 at 3W, 4W and also 5W.

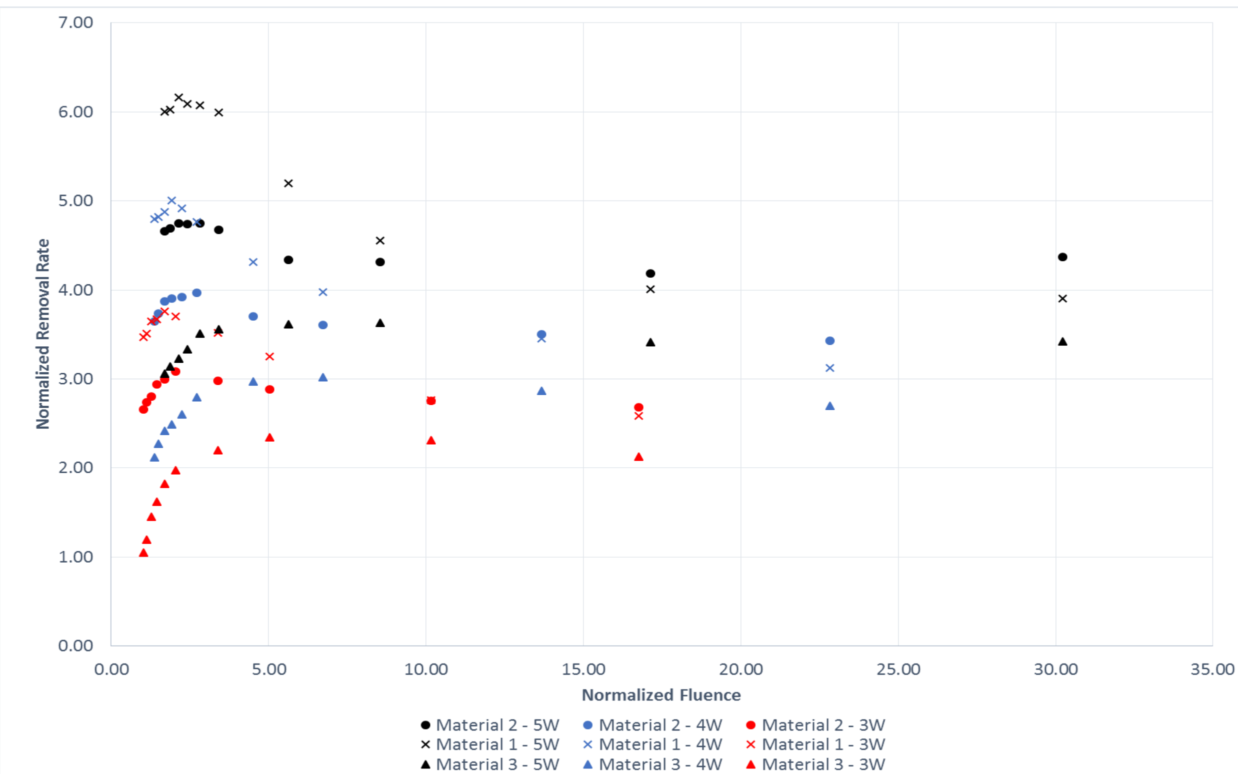


*Figure 6. Variation of the ablation rate with the fluence at three different average powers for Material 1 (1µm grain size, 80% wt diamond content), Material 2 (12µm grain size, 90% wt diamond content) and Material 3 (30µm grain size, 90% wt diamond content)*

### 5.3 Grain size influence

The maximum ablation rate is not connected to the optimal fluence for the three PCD grades at same average power, the maximum ablation rate shifts to higher fluence when PCD grain size increases. For example, at 4W, the optimal normalized fluence for highest ablation efficient is 1.93 for Material 1, 2.72 for Material 2 and 6.73 for Material 3. Higher fluence is required to achieve maximum ablation on grades with larger diamond grains. We can relate it to a difference of ablation threshold per material: ablation threshold is higher for material with larger diamond grains.

### 5.4 Diamond composition influence

At high fluence, some secondary effects must take place explaining why ablation rate of Material 1 drops whereas it remains constant for Material 2 and Material 3. At high fluence, it is observed that surface is rougher and some heat effects are visible. At higher fluence, over the optimal fluence, some energy is not used to ablate material and dissipated into the material heating it up. It can be assumed that the heat buildups participating in the ablation of material, and, as Material 2 contains more diamond, heat conduction is higher and secondary effect with heat are more important within Material 2 than Material 1 where these effect are lower and removal rate decreases.

## 6 Graphitization of Diamond under Ultra-Short Pulsed Ablation

### 6.1 Raman spectroscopy analyses

Studies demonstrated the occurrence of allotropic transformation of PCD after short-pulsed laser ablation[12,13]. During short pulsed laser ablation, as a thermal process, heat is transferred into diamond material, and diamond loses its crystalline structure and graphitizes when temperature increases over 700°C. A graphite layer is found to exist beneath the ablated top surface. Nonetheless, under ultra-short pulsed laser ablation, the graphitization process is more obscure, depending on the pulse length or fluence according to different papers[14,15,16]. The potential allotropic transformation of the diamond structure after laser ablation is a critical aspect for the development of a laser polishing process. Diamond structure is not affected through mechanical polishing[17], the PCD wafer product must conserve its diamond properties for tooling applications. Therefore, alternative laser polishing process must ensure integrity of the diamond structure after processing.

For that reason, as explained in D1.3, the carbon structure remaining on the surface after laser ablation is analyzed by Raman spectroscopy. Raman spectroscopy is a very suitable measurement method to characterize carbon structures present in a material as wavenumbers of different carbon structures are precisely defined[16]. Regarding the ultra-short pulsed ablation of PCD, the characteristic peaks are: the D band specific of crystalline diamond located at 1332cm$^{-1}$, the G band and the 2D band (or G' band) corresponding to graphite present at 1582cm$^{-1}$ and 2700cm$^{-1}$ respectively. Measurements are done using a Raman spectrometer Labram 300 from Horiba, Measurements are carried out at 532nm (higher peaks intensity at 532nm than at 650nm). Spectra are taken from 900cm$^{-1}$ to 2900cm$^{-1}$ on Material 1 and Material 2 grades to find any allotropic transformation difference between PCD grades after laser ablation. Measurement are taken on 5 areas (3x3 squares) from tests relative to the fluence variation carried out at 400fs like outlined by the table 4 below:

*Table 4. List of samples measured by Raman spectroscopy*

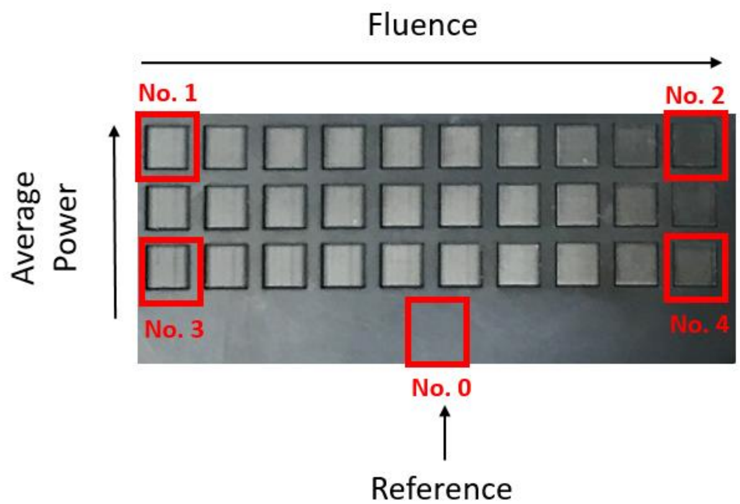


| | | |
|---|---|---|
| Area 0 | Reference point (initial surface) | Lapped surface for Material 1*****<br>EDM ground surface for Material 2***** |
| Sample 1 | High power – Low fluence | 5W – 1.70 |
| Sample 2 | High power – High fluence | 5W – 30.22 |
| Sample 3 | Low power – Low fluence | 3W – 1.01 |
| Sample 4 | Low power – High fluence | 3W – 16.76 |

*Material 1 and Material 2 are differently processed prior to polishing for industrial reasons. Material 1 is lapped with diamond grit whereas Material 2 is EDM ground with a copper electrode.

The Raman spectrometry measurements are repeated a Micro Raman spectrometer which is the combination of a Renishaw InVia Raman Spectrophotometer interfaced with JEOL scanning electron microscope to compare with results from the standard Raman spectrometer.

## 6.2 Standard Raman Spectrometer Measurements

Raman spectra of Material 1 and Material 2 from the standard Raman spectrometer are displayed from 1000cm$^{-1}$ to 1900cm$^{-1}$ on figure 7. Results over 1900cm$^{-1}$ do not show significant information: no 2D band characteristic of graphite are apparent at 2700cm$^{-1}$.

Diamond grit is used to lap the initial Material 1 surface before laser exposition. So the initial surface only contains diamond before laser exposition as represented on figure 7 (top) where only the D band characteristic of diamond at 1332cm$^{-1}$ appears. Then intensity of the D band reduces on the spectra of this same surface after various laser exposition. It implies a graphitization of diamond within Material 1 after laser ablation. The intensity of the D band is lower after laser radiation at 16.76 and 30.22 than at

1.01 and 1.70. So processing at low fluence transforms less the diamond crystalline structure into graphite, whereas the diamond structure has almost disappeared after processing at high fluence.

The spectrum of the initial Material 2 surface is different from the spectrum of the initial Material 1 surface: additional peaks are visible on figure 7 (bottom) and correspond to some copper deposited from the copper electrode on the Material 2 top surface during EDM sparking. After laser ablation, these peaks disappear proving the copper is only present on the top surface. Combined with this, the intensity of the D band is very low even at low fluence. Only at a power of 3W and a normalized fluence of 1.01, does the diamond structure remain. It appears that Material 2 is a more sensitive grade than Material 2 regarding graphitization. Material 2 contains a higher percentage of diamond than Material 1. Diamond having a higher thermal conductivity than cobalt, heat diffuses better into Material 2 which may participate in the increase of volume of graphitized diamond into the Material 2 compared to Material 1.

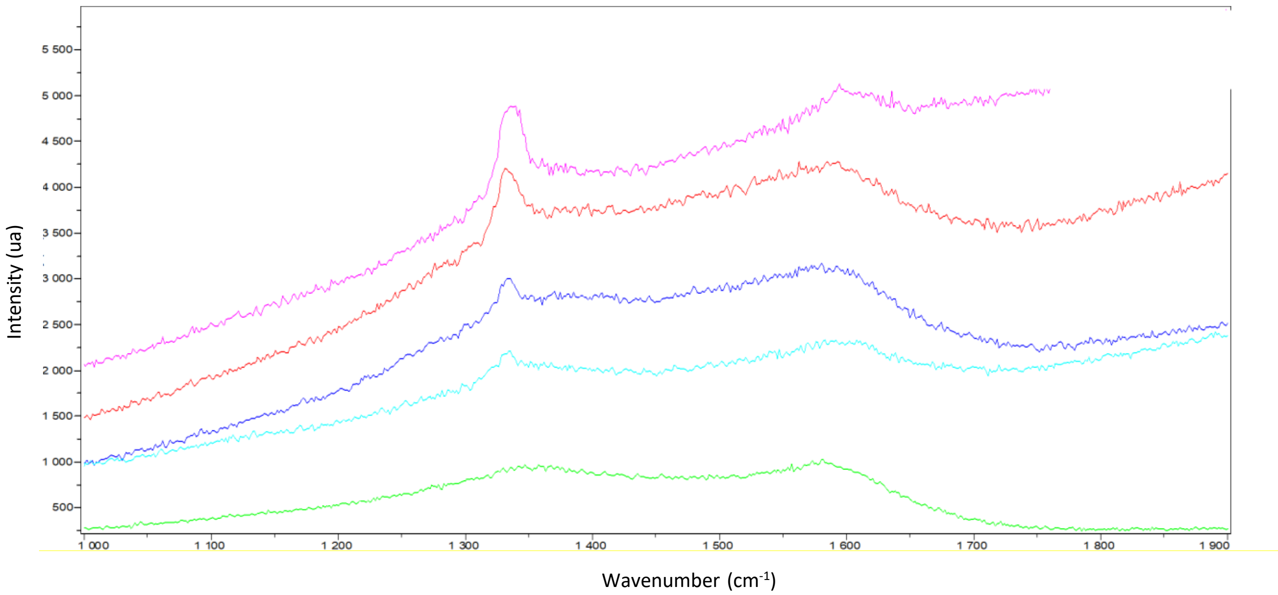


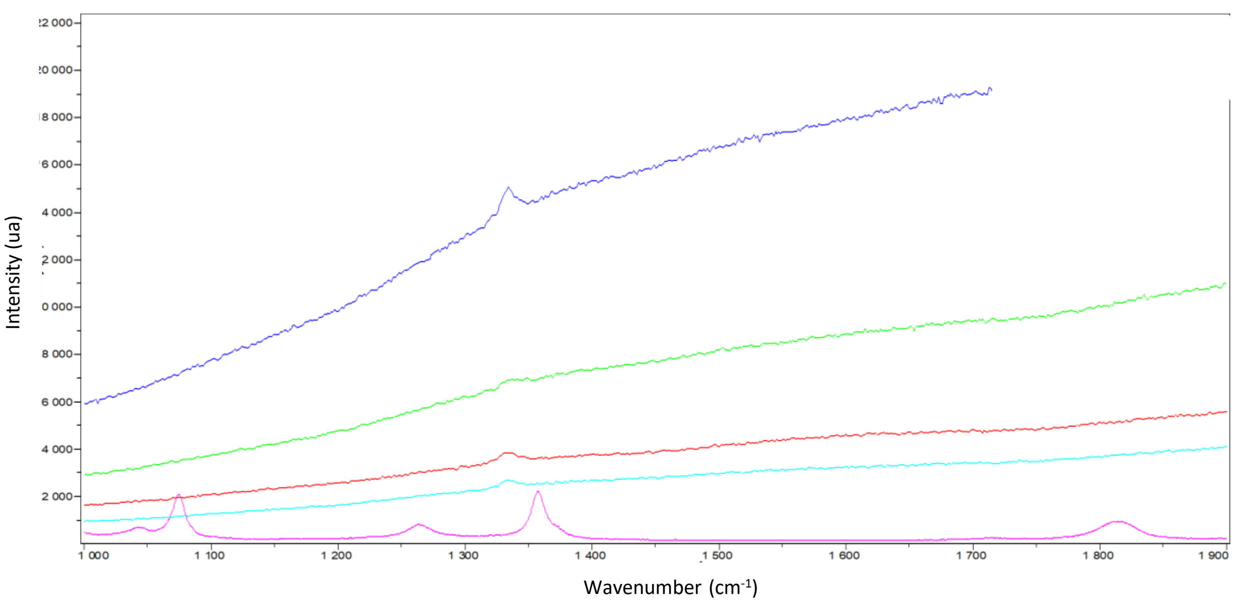


*Figure 7. (Top) Raman Spectra of Material 1 (1µm grain size, 80% wt diamond content) and (bottom) Material 2 (12µm grain size, 90% wt diamond content) – Red: Sample 1 (5W – 1.70);*

*Cian: Sample 2 (5W – 30.22); Blue: Sample 3 (3W – 1.01); Green: Sample 4 (3W – 16.76); Purple: Area 0 (lapped)*

## 6.3 Micro Raman Spectrometer Measurements

Raman spectra from Micro Raman spectrometer are shown from 1100cm$^{-1}$ to 1900cm$^{-1}$ as there is no significant peak over 1900cm$^{-1}$ (Fig.8).

The level of chemical information delivered by Micro Raman spectroscopy is much higher than standard Raman spectrometer: whereas no possible conclusion regarding graphite G band was possible after standard Raman spectroscopy, G bands corresponding to graphite structure are well defined at 1582cm$^{-1}$ at 3W/16.76 and at 5W/30.22 on figure 8 (top). Besides the D bands are not as sharp as the reference surface diamond structure and are slightly shifted to lower wavenumber. The remaining diamond structure is also altered: the crystalline structure contains some defects. However, no D band are present at 3W/1.01 and at 5W/1.70. It fully confirms that only the fluence is responsible for graphitization of the diamond and that the average power has no influence. Analysis with the micro Raman spectrometer will be repeated on other grades to confirm its advantages compared to a classic Raman spectrometer.

However, micro Raman spectra of Material 2 after laser oblation is similar to the spectra obtained with standard Raman spectrometer: no G band are observable on figure 8 (bottom) like micro Raman spectrometry analyses revealed for Material 1. Only the micro Raman spectrum of the initial Material 2 surface shows a G band at 1582cm$^{-1}$. Graphitization of the diamond occurs during grinding EDM but this is not the interest of the project. The micro Raman spectra of Material 2 surfaces after laser ablation only confirm results from standard Raman spectra but do not deliver additional information. The reason for the difference of micro Raman results between Material 1 and Material 2 is unknown and is not the scope of this project.

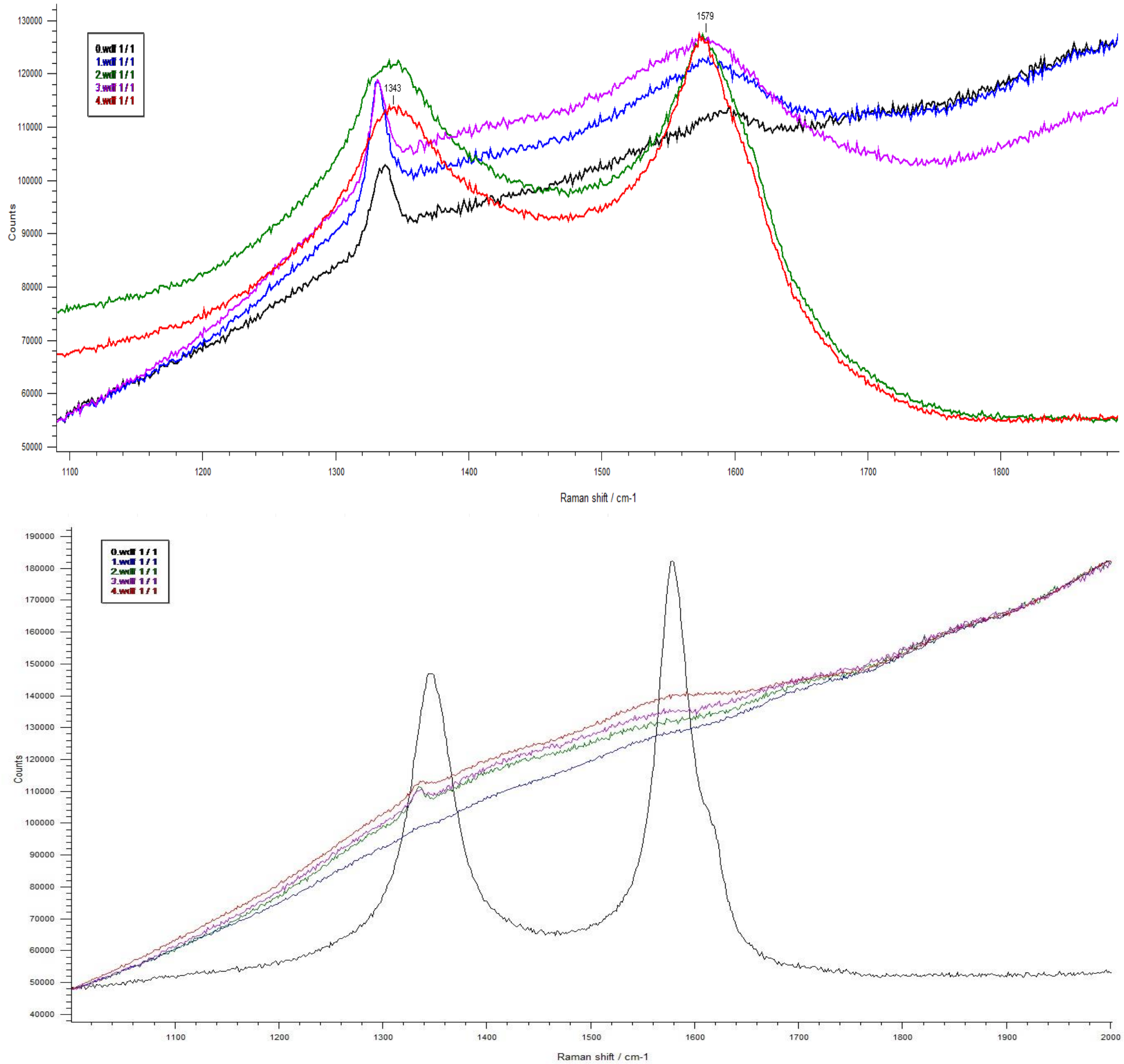


*Figure 8. (Top) Micro Raman Spectra of Material 1 (1µm grain size, 80% wt diamond content) and (bottom) Material 2 (12µm grain size, 90% wt diamond content) – Blue: Sample 1 (5W – 1.70); Green: Sample 2 (5W – 30.22); Purple: Sample 3 (3W – 1.01); Red: Sample 4 (3W – 16.76); Black: Area 0 (lapped/EDM ground)*

# 7 Conclusion

After the system specifications stated in deliverable D1.2 explaining the requirement for high average power of 200W and ultra-short pulse below 500fs to achieve KIP1 (Tab.1), studies involved in T2.3 and exposed in this deliverable D2.3 highlights specific characteristics of the process and system as well as some limitations.

The process will have to be adapted to the different PCD grades as the removal rate differs between PCD grades. Graphitization of the diamond surface can occur after laser ablation at high fluence. Therefore, final processing step must be executed at low fluence. All the detailed specifications of the developed process are listed in table 5.

Two limitations have been identified: the focal lens and the scanning device. Considering optical device available, the smallest achievable spot size is 7.6µm which will probably be higher than roughness peak width. This remains to be fully assessed after processing at high average power. Heat accumulations effects cause severe surface damage at high spot overlap. After evaluation of the spot size required for the process, the limitation in scanning speed is a concern regarding overlap to be achieved and potential surface damage. Strategy must be considered to prevent such thermal effects.

*Table 5. Final specifications of ultra-fast high power system to meet Element Six KPIs regarding laser polishing process of PCD*

| Parameters | Current Performances | E6 Specifications | Specification agreed with partners |
|---|---|---|---|
| Wavelength | 1030nm | 1030nm | 1030nm |
| Power | 5W | 200W | 150W* |
| Pulse duration | 230fs – 10ps | < 500 fs – 10ps | 400fs – 10ps |
| Frequency | 60kHz-1MHz | <2MHz | <2MHz |
| $M^2$ | 1.2 | 1.2 | <1.3 |
| Pulse burst | None | Pulse burst | Multi pulses burst |
| Maximum scanning speed | 3000mm/s | <3000mm/s | 3000mm/s |
| Spot diameter | 20µm | 2µm – 160µm | 7.6µm - 160µm |
| Polarization | Circular | Circular | Circular |

# 8 References

[1] Weikert M., Dausinger F., “Cutting of diamond”, in Dausinger F., Lubatschowski H., Lichtner F., [Femtosecond technology for technical and medical applications], Springer, Berlin/Heidelberg, 155 – 165 (2004).

[2] Joswig A., Risse S., Eberhardt R., Tünnermann A., “Laser generated and structured prototypes of diamond too tips for micro optics fabrication”, Proc. American Society for Precision Engineering 31, 53–56 (2010).

[3] Eberle G., Dold C., Wegener K., “Laser fabrication of micro-cutting tool-related geometries using a high numerical aperture micro-scanning system”, The International Journal of Advanced Manufacturing Technology, 81(5-8), 1117 – 1125 (2015).

[4] Neuenschwander B., Jäggi B., Schmid M., Rouffiange V., Martin P.E., “Optimization of the volume ablation rate for metals at different laser pulse-durations from ps to fs”, Proc. SPIE 8243 (2012).

[5] Neuenschwander B., Jäggi B., Schmid M., Hunziker U., Luescher B., Nocera C., “Processing of industrially relevant non-metals with Laser pulses in the range between 10 ps and 50 ps”, Proc. ICALEO Paper M103 (2011).

[6] Neuenschwander B., Jäggi B., Schmid M., “From ps to fs: Dependence of the Material Removal Rate and the surface Quality on the Pulse Duration for Metals, Semiconductors and Oxides”, Physics Procedia 41, 794-801 (2013).

[7] Neuenschwander B., Jäggi B., Schmid M., Hennig G., “Surface structuring with ultra-short laser pulses: Basics, limitations and needs for high throughput”, Physics Procedia 56,1047-1058 (2014).

[8] Weber R., Graf T., Berger P., Onuseit V., Wiedenmann M., Christian Freitag, and Anne Feuer, “Heat accumulation during pulsed Laser materials processing”, Optics Express 22(9), 11312 – 11324 (2014).

[9] Weber R., Graf T., Freitag C., Feuer A., Kononenko T. and Konov V. I., “Processing constraints resulting from heat accumulation during pulsed and repetitive laser materials processing”, Optics Express, 25(4), 3966 – 3979 (2017).

[10] Christensen B. H., Vestentoft K., Balling P., “Short-pulse ablation rates and the two temperature model”, Applied Surface Science 253(15), 6347 – 6352 (2007).

[11] Pacella M., Axinte D. A., Butler-Smith P. W., Daine M., “On the topographical/chemical analysis of polycrystalline diamond pulsed laser ablated surfaces”, Procedia CIRP 13, 387 – 392 (2014).

[12] Butler-Smith P.W., Axinte D.A., M. Pacella, Fay M.W., “FIB/TEM/EELS micro/nanometric investigations of the effects of laser ablation on the diamond/binder structure in polycrystalline diamond composites”, Journal of Materials Processing Technology 214(5), 1153–1161 (2014).

[13] Ohfuji H., Okuchi T., Odake S., Kagi H., Sumiya H., Irifune T., “Micro-/nanostructural investigation of laser-cut surfaces of single- and polycrystalline diamonds”, Diamond & Related Materials 19(7-9), 1040–1051(2010)

[14] Eberle G., Jefimovs K., Wegener K., “Characterisation of thermal influences after laser processing polycrystalline diamond composites using long to ultrashort pulse durations”, Precision Engineering 39(2), 16 – 24 (2015).

[15] Eberle G., Wegener K., “Ablation study of WC and PCD composites using 10 picosecond and 1 nanosecond pulse duration at green and infrared wavelengths”, Physic Procedia 56, 951 – 962 (2014).

[16] Kononenko V.V., Kononenko T.V., Pimenov S.M., Sinyavskii M.N., Konov V.I., Dausinger F., “Effect of the pulse duration on graphitisation of diamond during laser ablation”, Quantum Electronics 35(3), 252 – 256, (2005).

[17] Chen Y., Zhang L. C., “Polishing of Diamond Materials”, Engineering Materials and Processes, Springer-Verlag London (2013).